SNOW COVER REMOTE SENSING AND SNOWMELT RUNOFF FORECASTS IN THE SPANISH PYRENEES USING THE SRM MODEL

E. Gómez-Landesa and A. Rango
USDA-ARS Hydrology Laboratory
Beltsville, Maryland, USA

ABSTRACT

Snowmelt runoff forecasts are being carried out using the SRM model in several basins of the Spanish Pyrenees. These results are being used by hydropower companies of Spain for a reasonable management of water resources. We describe a method for snow mapping using NOAA-AVHRR data and a procedure to retrospectively estimate the accumulated snow water equivalent volume with the SRM model. A linear combination of NOAA channels 1 and 2 is used to obtain a snow cover image in which the product is the percent of the snow covered area in each pixel. Real-time snowmelt forecasts are being carried out with the Snowmelt Runoff Model (SRM) using the snow covered area as an input. Even in basins with a total absence of historical discharge and meteorological data, the SRM model provides an estimation of the snowmelt daily discharge. Integrating the forecasted streamflow over the recession streamflow, the snowmelt volume is obtained as a function of time. This function converges asymptotically to the net stored volume of water equivalent of the snowpack.

INTRODUCTION

The study of snowmelt water resources in the Spanish Pyrenees using satellite remote sensing started in the year 1991 with an agreement between individual hydropower companies and the government. Before using satellite remote sensing, the estimation of snowmelt water resources in the Spanish Pyrenees had been carried out by the Spanish government by setting up a number of snow depth stakes at several points. From manual measurements of snow depth and snow density together with the altitude at these points, one must use statistical correlations in order to estimate the snow water equivalent. This method is still used, but it is expensive and not very accurate due to the fluctuations of the spatial distribution of snow. Satellite remote sensing appears to be a more efficient solution than terrestrial observations.

Based on the specific needs of the hydropower companies, 18 main basins were identified on the Spanish side of the Pyrenees, containing a total of 42 flow measuring points. Two experimental basins are also being studied, one in Cordillera Cantabrica (North of Spain) and another one in Sierra Nevada (South of Spain). The repeat period of the NOAA

satellites can provide three or four images a day of the same area, thus allowing a daily monitoring of the snow covered area, except when this area is cloud covered. Some of the basins are as small as 10 km², while the AVHRR spatial resolution is approximately 1.1 km² at nadir, and increases with the distance from it. Thus, it is not possible to apply a snow-non snow classification based on NOAA images in such small basins, and it is necessary to work at sub-pixel levels.

The snow cover for each basin is obtained from a lineal combination of channel 1 (visible) and channel 2 (near infrared) of NOAA-AVHRR. Both channels are previously normalized (geometric and radiometric corrections are performed) and a UTM resample is necessary due to a discontinuity of the Pyrenees area on the ordinary UTM grid. Each pixel of the resulting combined image contains the snow cover percent of its corresponding area. The coefficients of the lineal combination depend slightly on the albedo variations of snow and ground. To verify this method, several Landsat TM images of the same geographic window (Pyrenees area) and approximately the same day were used. Correlations between NOAA snow cover images and Landsat TM multichannel classifications of snow were always greater than 0.9.

A digital elevation model (DEM) is used together with the snow cover image of each basin to obtain an hypsometric table which contains the percent of snow covered area in each elevation range of the basin. Snow hypsometric tables are generated once each 15 days (approx.) during the whole year, and more frequently during the melting season (April to June). Recent improvements of the snow mapping are being developed using consecutive NOAA images in order to find more accurately the shapes of snow patches.

Monitoring the snow cover with time allows production of the so-called *snow depletion curves* for each basin (Martinec *et al.*, 1998). These curves are used together with meteorological data as input variables for the Snowmelt Runoff Model (SRM). Even in basins with a total absence of historical discharge and meteorological data, the SRM model provides an estimation of the daily snowmelt discharge. The model parameters of these ungauged basins are obtained indirectly from criteria such as the basin size, proximity of other gauged basins and shape similarities with gauged basins.

The snowmelt streamflow of each basin is the integrated over the recession streamflow, obtaining the snowmelt volume as a function of time. This function converges asymptotically to the accumulated daily discharge, which is converted into the stored volume of water equivalent using the losses reflected in the runoff coeffient. If the snow density is known, the stored volume of the snowpack can also be obtained.

Future improvements of the snow water equivalent estimation may be carried out using microwave remote sensing of brightness temperature of snow together with the radiative transfer theory applied to the snow layer. Some ongoing microwave experiments will hopefully reveal the possibilities of these bands in operational snow hydrology (Hallikainen, 1998).

SNOW COVER MAPPING

A lineal combination of NOAA-AVHRR channels 1 and 2 is being used to obtain the snow cover of the Pyrenees basins. Orbital geometric and atmospheric radiometric corrections are performed on the NOAA raw data received by the Remote Sensing Laboratory of the University of Valladolid (Spain) and the semi-processed product is then sent to the USDA-ARS Hydrology Laboratory (Beltsville, Maryland, USA). Both channels 1 and 2 receive

reflected sunlight, the first one in the visible spectrum and the second one in the near infrared, with slight differences between the spectral response of AVHRR sensors of the four NOAA operative platforms (NOAA 10, 11, 12 and 14). NOAA 14 is preferred because of its noon orbit over the Pyrenees area. Based on the snow and ground albedos, the combination *Im* of channels 1 and 2 is given by the simple equation:

$$Im = a_1C_1 + a_2C_2 \qquad (1)$$

where an C_1 and C_2 are the pixel values of channels 1 and 2 repectively. To find the combination coefficients a_1 and a_2, the following condition is imposed:

$$a_1\begin{pmatrix} S_1 \\ G_1 \end{pmatrix} + a_2\begin{pmatrix} S_2 \\ G_2 \end{pmatrix} = \begin{pmatrix} 255 \\ 0 \end{pmatrix} \qquad (2)$$

where 255 is the maximum value of an image with 8 bits per pixel. S_1 and S_2 are the minimum snow thresholds of channels 1 and 2 respectively. The interpretation of these thresholds is as follows (see Figure 1): a pixel value greater than or equal to S_1 corresponds to a fully-covered snow area in channel 1 (the same can be said for channel 2). In the same way, G_1 and G_2 are the maximum ground thresholds in each channel, so that a pixel value lower than or equal to these thresholds corresponds to a snow free area. Pixels between these values are mixed pixels of snow and ground in different percents. These percents can be found using Equations (1) and (2). A lineal behavior of the mixed pixels of channels 1 and 2 (Figure 1) leads to a lineal behavior of the combined image, given that Equation (1) is lineal as well (Landesa, 1997).
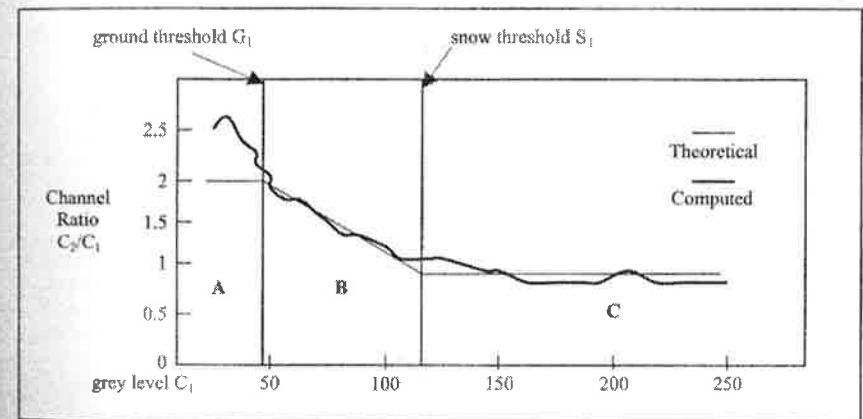

Figure 1: Channel ratio C_2/C_1 as function of C_1.

Figure 1 represents the ratio of channel 2 to channel 1 as a funtion of channel 1. Zone A contains bare ground pixels which verify $C_1 < G_1$. Zone C contains full-covered snow pixels which verify $C_1 > S_1$. Zone B contains mixed pixels of snow and ground which verify $G_1 < C_1 < S_1$. Representing C_2/C_1 as a function of channel 2, a similar graph to this one is obtained, leading to the same analysis.

Snow and ground thresholds were obtained by classification in both channels, comparison with Landsat images and ground observations. Changes in snow and ground albedo produce differerent thresholds, so that the classifications must be repeated once a month. During the melting season it is convenient to repeat the classifications once a week, due to the rapidly changing snow albedo values. Using these thresholds, from Equation (2) the coefficients a_1 and a_2 are obtained as

$$a_1 = 255\left(\frac{G_2}{S_1 G_2 - S_2 G_1}\right)$$

$$a_2 = -255\left(\frac{G_1}{S_1 G_2 - S_2 G_1}\right)$$

(3)

Each pixel of the snow cover image is then obtained from the pixel values of channels 1 and 2 using

$$Im = C_1 a_1 + C_2 a_2 = 255\left(\frac{C_1 G_2 - C_2 G_1}{S_1 G_2 - S_2 G_1}\right)$$

(4)

Of course, assuming a lineal behaviour of C_1 and C_2, this equation leads to 255 in case of snow cover and to 0 in case of bare ground, but also returns a pixel value proportional to the snow covered area in case of a mixed pixel. It can be verified assuming a percent p of snow cover inside an arbitrary pixel, so that

$$C_1 = pS_1 + (1-p)G_1$$
$$C_2 = pS_2 + (1-p)G_2$$

(5)

together with Equation (4), returns a grey level $255p$, which is directly proportional to the percent p of snow covered area.

It is unnecessary to add a constant coefficient to Equation (1). Statistical optimization of the correlation coefficient between NOAA and Landsat snow cover images gives a constant coefficient on the order of 10^{-2}, which produces a negligible effect on the grey levels of the resulting combination. At the same time, a constant value does not contribute real information and has no physical significance and therefore shall be avoided.

An example of this combination can be seen in Figure 2, which corresponds to a NOAA image of the Pyrenees on 21 March 1998. As a result of the lineal combination of channels 1 and 2 (Figures 2a and 2b), a snow covered image is obtained in which the ground appears with a value 0 (Figure 2c). Water is often present with a low grey level due to water vapour.

Taking ground control points on these images, a polynomial is obtained to resample an image into UTM coordinates. It is enough to apply a first order polynomial given that a previous orbital correction has been performed. Since there is a discontinuity in the UTM grid on the Pyrenees (it changes from grid 30 to grid 31), a new grid was defined with its center at the meridian $0°$ $30'$ East. To apply an extension of the ordinary grids 30 or 31 to the whole Pyrenees is not the best solution; it has been calculated that this extension increases the maximum lineal deformation of the UTM proyection from 1.0004 to 1.0037, multiplying the maximum deformation almost nearly by 10 (Landesa, 1997).

The snow cover of each basin is obtained using a Digital Elevation Model (DEM) of each basin. Since each basin has a different size, the DEM area resolution varies from 650 m^2 to 13,800 m^2. The DEM altitude resolution is 20 m in all the basins. A snow hypsometric table (snow cover versus elevation) is generated for each basin with an elevation range of 100 m.

Figure 2a. Channel 1
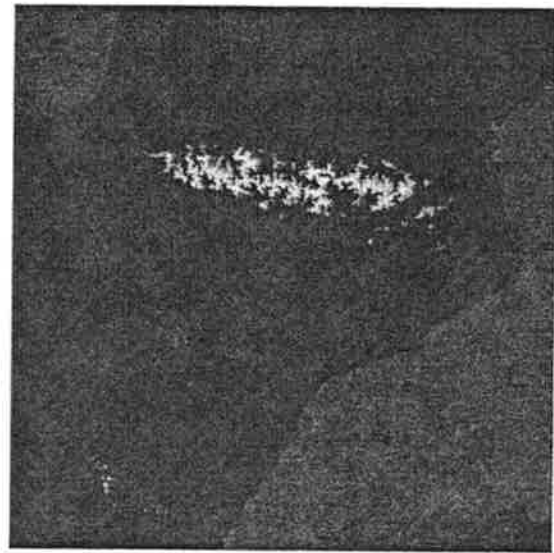
Figure 2b. Channel 2

Figure 2c. Snow cover image

Figure 2: NOAA-14 image of the Pyrenees on 21 March 1998.

Figure 3 (see page 309), left side, shows an image of Cinca Basin at the central Pyrenees (798.1 km^2). This window has been extracted from a snow covered image of 10 March 1998. It can be seen that different grey levels correspond to different percents of snow and ground. The basin border is displayed in red color and the streams in green color. The image at the right side shows the DEM of the same basin, displaying an arbitrary color palette.

SNOWMELT RUNOFF FORECASTING

The snow cover of each basin is one of the input variables of the Snomelt Runoff Model (SRM or Martinec-Rango model), which can easily be run on a desktop computer (Baumgartner and Rango, 1991). Snowmelt runoff simulations and forecasts were performed using this model in 42 mountain basins of the Spanish Pyrenees. Figure 4 shows the 1998 snowmelt forecast of the NR4 basin at the central Pyrenees. These results are being used by the Spanish power companies to improve water management.
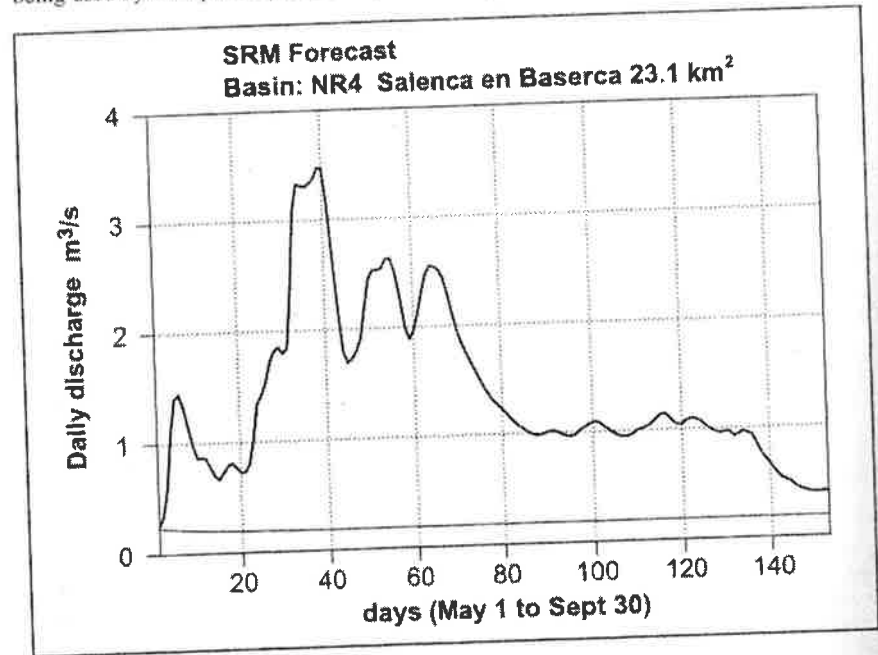

Figure 4: *Snowmelt runoff forecast for NR4 basin. 1998.*

The SRM model computes the daily discharge from snowmelt and from rainfall of several elevation zones of a basin. It has three input variables (snow cover, temperature and precipitation) and eight parameters to adjust using historical measurements of the basin and hydrological considerations (Martinec et al., 1998).

In this work, the Pyrenees basins have an approximate elevation range of 2,500 m.a.s.l. (usually from 700 to 3200 m) and are divided into 5 or 6 elevation zones of 500 m each. Temperature and precipitation are extrapolated by the SRM computer code from a reference metorological station to each elevation zone. Snow input is introduced by means of the *Snow Depletion Curves*, which are obtained from the snow cover mapping method described previously.

Running the model in the forecasting mode, a daily discharge is obtained for each basin. The forecast period is usually five months, from 1 May to September 30, which includes the snow melting season. Since a long term precipitation forecast is not available for the Pyrenees, the method used is to run the model in absence of rainfall and with historical

temperatures. The snow input is extrapolated using the so-called *Modified Depletion Curves* (MDC) (Martinec *et al.*, 1998). The resulting runoff (Figure 4) includes snowmelt and the recession flow of the basin. To calculate the volume V(t) of melted snow, the forecasted flow Qa(t) is integrated over the recession flow Qb(t):

$$V(t) = \int_0^t [Qa(s) - Qb(s)]ds \qquad (6)$$

Figure 5 shows the net accumulated snowmelt volume as a function of time. This is the snowmelt volume that flows through the measuring point of the basin. To obtain the water equivalent of stored snow, this volume is corrected using the runoff coefficient of the basin. The snow volume may be obtained if the snow density is known.
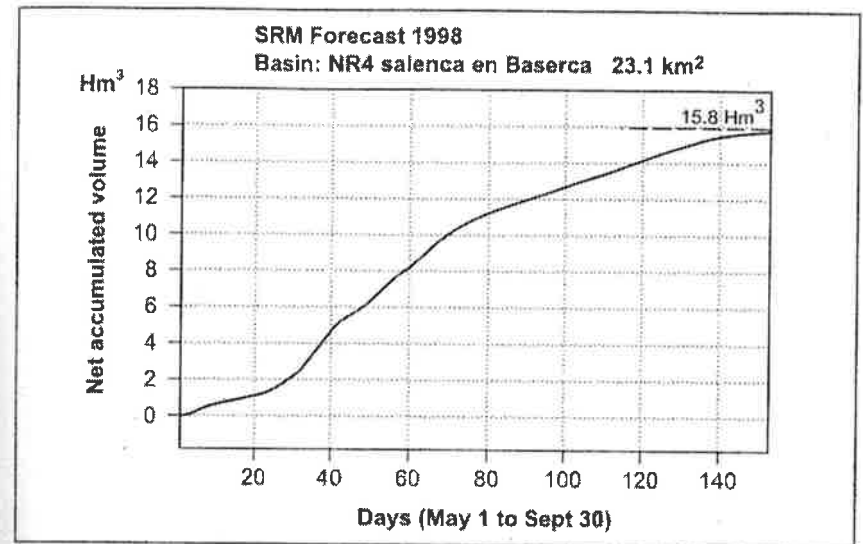

Figure 5: *Net snowmelt accumulated volume.*

DISCUSSION

Water equivalent estimation can be improved using microwave remote sensing techniques. It has been shown that satellite microwave data can be used to obtain information about the average basin snow-water equivalent (Rango *et al.*, 1989). The advantage of these frequencies is the possibility of snow mapping of cloud-covered areas (Nagler and Rott, 1992). It is not yet ready as an operational method due to difficulties concerning poor spatial resolution in the case of passive microwave instruments, and image interpretation in the case of active instruments.

In both active and passive remote sensing, a number of models and computer codes have been developed by researchers to simulate snow behavior and many interesting features emerge from the different numerical simulations (Kong, 1989). Different models based on rather different physical mechanisms often provide more or less the same correct answer (O'Neill, 1996). Improvements of future remote sensing instruments will hopefully lead to the use of microwave frequencies in snow hydrology.

REFERENCES

Baumgartner, M.F. and A. Rango, 1991. *Snow cover mapping using microcomputer image processing systems.* Nordic Hydrology, 22, 1991. pp. 193-210.

Hallikainen, M. 1998. *HUT Annual Report 1997*, Laboratory of Space Technology. Helsinki University of Technology, Finland.

Landesa, E.G. 1997. *Evaluación de recursos de agua en forma de nieve medianteteledetección usando satélites de la serie NOAA. (Estimation of snow water resources using remote sensing with NOAA satellites).* Doctoral Thesis, Chapter VII. ETS Ingenieros de Caminos, Canales y Puertos. UPM. Madrid. Spain.

Martinec, J., A. Rango, and R. Roberts, 1998. *Snowmelt Runoff Model (SRM) User's Manual.* Geographica Bernensia. Department of Geography, University of Bern, Switzerland.

Nagler, T., and H. Rott, 1992. *Development and intercomparisons of snow mapping algorithms based on SSM/I data.* IGARSS'92 Vol I, pp 812-814.

O'Neill, K. 1996. *The State of the Art of modelling millimeter-wave remote sensing of the environment.* Special Report 95-25. Department of the Army, Corps of Engineers, New Hampshire, USA.

Rango, A., J. Martinec, A.T.C. Chang, J.L. Foster, and V.F. Katwijk, 1989. IEEE Transactions on Geoscience and Remote Sensing. Vol. 27, No 6, November 1989.

Kong, J.A. 1989. *Radiative transfer theory for active remote sensing of two layer random medium.* Electromagnetics Research (PIER1). New York: Elsevier. USA.

APPLICATIONS OF

REMOTE SENSING

IN HYDROLOGY

L'APPLICATION DE LA TÉLÉDÉTECTION EN HYDROLOGIE
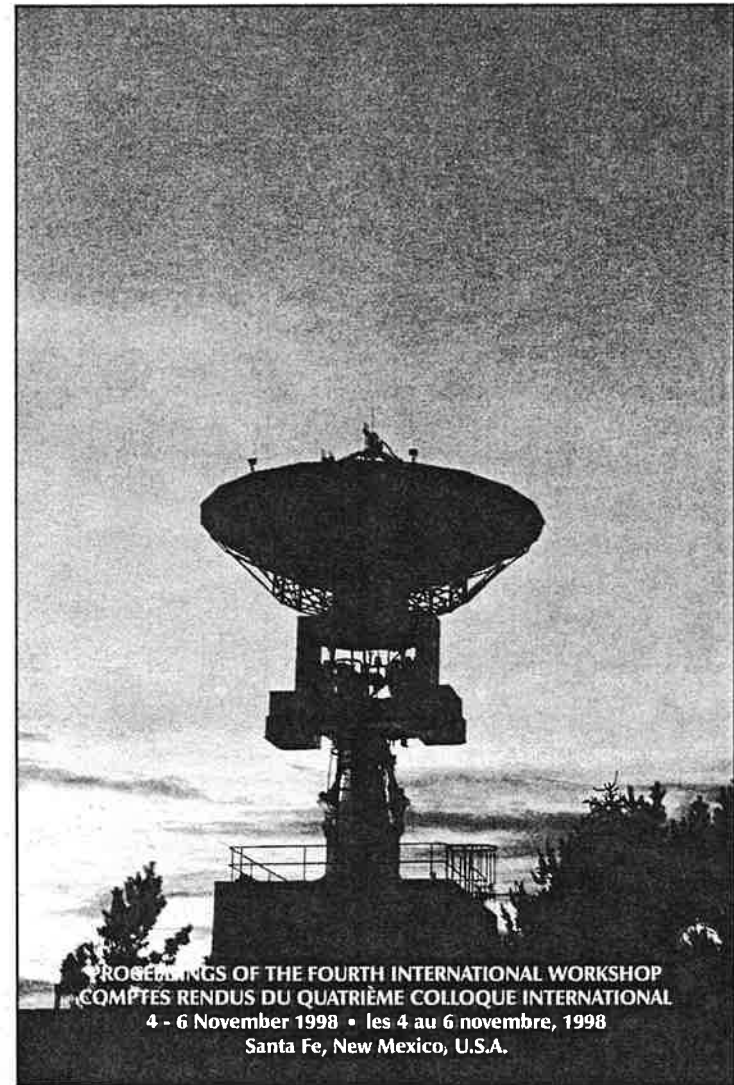
PROCEEDINGS OF THE FOURTH INTERNATIONAL WORKSHOP
COMPTES RENDUS DU QUATRIÈME COLLOQUE INTERNATIONAL
4 - 6 November 1998 • les 4 au 6 novembre, 1998
Santa Fe, New Mexico, U.S.A.

Rédacteurs A. Pietroniro, R. Granger, T.J. Pultz, Editors